The Effects of Compressibility on the Propagation of Premixed Deflagration

A. Fecteau & J. McDonald & A. Sow & M. Radulescu
University of Ottawa
Ottawa, Ontario, Canada

1 Introduction

The transition from deflagration to detonation (DDT) is an important process to avoid costly disasters in the petrochemical industry. Example of such a disaster are the 2005 Hertfordshire oil storage terminal fire or the 1970 propane vapour cloud explosion in Port Hudson. Such events have far-reaching disastrous consequences due to the overpressures created by detonation waves. It is well-known that in experimental and numerical premixed flames, the flame front is rarely planar and quickly forms a cellular structure with cusp-like sections between the cells. These instabilities in the flame front have the effects of increasing the flame velocity. Under the quasi-isobaric, near-equidiffusional ($Le \to 1$) and infinite activation energy ($E_a \to \infty$) approximation, Darrieus [1] and Landau [2] have predicted independently that, in a premixed combustion, the cellular flame front would be unconditionally unstable with a growth rate proportional to the wave number as,

$$\bar{\sigma} = \bar{k}\bar{u}_1 \frac{\Theta_2}{1+\Theta_2}\left(\left(1+\Theta_2-\frac{1}{\Theta_2}\right)^{1/2}-1\right), \tag{1}$$

where $\bar{\sigma}$ is the growth rate of the perturbances, $\Theta_2 = 1+Q$, Q the heat release of reaction, $\bar{u}_1$ is the velocity of the flame and $\bar{k}$ is the wave number of the perturbation.

Moreover, Clavin and Williams [3] and Peke and Clavin [4] accounted for the first-order correction to the quasi-isobaric flames from the effect of the flame thickness or thermal-diffusive ratios and showed that the flame thickness has a stabilizing effect. Further analytical work [5–8] and numerically studies [7–12] have reaffirmed that this effect of the flame structure has a stabilizing effect. They also have shown that reducing the Lewis number increases the instability and the sensitivity to the energy of activation and that the Prandtl Number and ratio of specific heats does not have a significant effect on the flame stability.

The effect of compressibility on the instability of premixed flames was then studied analytically in the linear regime by Travnikov et al. [6]. They showed that not only does the growth rate of a fast flame increase with the flame velocity, but the range of unstable wavelengths is also increased. Further numerical investigation by Travnikov et al. [9] confirmed the growth rate in the linear region that was found in his

previous paper were correct. He also demonstrated that, in the compressible regime, the growth rate is affected by the precompression region in the unburned gases. Further analytical studies done by He [13] and Bychkov [14] have shown the instability in the linear domain rapidly disappears when approaching the CJ deflagration velocity. To confirm these new findings and to enhance the understanding of the effect of the compressibility on fast flames, this study systematically examines the effects of compressibility on the growth rate and propagation velocities of cellular flames by increasing the flame Mach number from the quasi-isobaric flame velocity to the Champan-Jouget deflagration velocity.

2 Numerical Model

In order to simulate the hydrodynamics of a deflagration flame, the compressible Navier-Stokes equations are used, coupled with the 1-step model to simulate the non-equilibrium hydrodynamics of the system using the MG code developed by Mantis Ltd. [15]. The governing equations are the conservation of mass,

$$\frac{\partial \rho}{\partial t} + \frac{\partial \rho u_j}{\partial x_j} = 0, \tag{2}$$

conservation of momentum,

$$\frac{\partial \rho u_i}{\partial t} + \frac{\partial \rho u_i u_j}{\partial x_j} = -\frac{\partial p}{\partial x_i} + \frac{\partial \sigma_{ij}}{\partial x_j}, \tag{3}$$

conservation of energy,

$$\frac{\partial \rho e}{\partial t} + \frac{\partial \rho u_j e}{\partial x_j} + \frac{\partial p u_j}{\partial x_j} = \frac{\gamma}{\gamma - 1}\frac{\partial^2 T}{\partial x_j \partial x_j} + \frac{\partial u_j \sigma_{ij}}{\partial x_i} + QW, \tag{4}$$

species transport,

$$\frac{\partial \rho Y}{\partial t} + \frac{\partial \rho u_j Y}{\partial x_j} = \frac{1}{Le}\frac{\partial^2 Y}{\partial x_j \partial x_j} - W. \tag{5}$$

Where, the non-dimensional stress tensor is given by $\sigma_{ij} = Pr\left(\frac{\partial u_i}{\partial x_j} + \frac{\partial u_j}{\partial x_i} - \frac{2}{3}\delta_{ij}\frac{\partial u_k}{\partial x_k}\right)$ and the reaction rate is $W = A\rho Y e^{-E_a/T}$. The non-dimensional variables are scaled using the following scheme:

$$x_x = \frac{\bar{\rho}_1 \bar{V}_1 \bar{c}_p \bar{x}_x}{\bar{k}}, \quad x_y = \frac{\bar{\rho}_1 \bar{V}_1 \bar{c}_p \bar{x}_y}{\bar{k}}, \quad t = \frac{\bar{\rho}_1 \bar{V}_1^2 \bar{c}_p \bar{t}}{\bar{k}}, \quad u = \frac{\bar{u}}{\bar{V}_1}, \quad v = \frac{\bar{v}}{\bar{V}_1},$$
$$\rho = \frac{\bar{\rho}}{\bar{\rho}_1}, \quad e = \frac{\bar{e}}{\bar{V}_1^2}, \quad p = \frac{\bar{p}}{\bar{\rho}\bar{V}_1^2}, \quad T = \frac{\bar{R}_g \bar{T}}{\bar{V}_1^2}, \quad \mathrm{Pr} = \frac{\bar{\mu}\bar{c}_p}{\bar{k}},$$
$$\mathrm{Le} = \frac{\bar{k}}{\rho \bar{c}_p \bar{\lambda}}, \quad \Lambda = \frac{\bar{k}\bar{A}}{\bar{\rho}_1 \bar{V}_1^2 \bar{c}_p}, \quad E_a = \frac{\bar{E}_a}{V_1^2}, \quad Q = \frac{\bar{Q}}{V_1^2}, \quad Y = \frac{\bar{Y}}{Y_1},$$

where an overbar denote dimensional properties unless indicated otherwise. In these expressions, t is the time, x_i is the space vector, ρ is the density, u_i is the velocity vector, V_1 is the velocity of the planar flame, p is the pressure, e is the specific kinetic and thermal internal energy, T the temperature, A is the mass fraction of reactants, k is the thermal conduction constant, c_p the heat capacity, E_a is the activation energy, γ is the ratio of specific heats, λ is the diffusion coefficient, R_g is the real gas constant, T is the temperature, Q_n is the heat release of reaction, Pr is the Prandl number, Le is the Lewis number, Y is the fraction of reactants and Λ is the pre-exponential value of the reaction rate.

3 Numerical Setup

In this section, the numerical setup and its significance of the results are discussed. Sharpe [8] has shown that the length of ± 2000 for the quasi-isobaric cases is sufficient even if the pressure waves reach the boundaries. Further studies on the domain length for the compressible regime show that a domain length of ± 2000 is acceptable. To study the evolution of fast flames in their intrinsic cellular state, the domain width have to be such that the deflagration exhibit cellular growth within the domain, while also limiting the width of the domain to negate cell-cell interactions, as they are not the main interest of this paper. We chose the domain width to be 16.5, for all problems stated above, to be approximately half the maximum growth-rate wavelength of the most stable or quasi-isobaric case (Problem 1), the maximum growth rate was found using the isobaric linear stability analysis by Liberman [5]. We chose this to minimize the risk of having a domain width that stabilizes the flame back to a planar state and to minimize the computation time required to get the evolution of the stiffest cases, due to the low Mach numbers. The choice of boundary condition is important for numerical accuracy and to minimize their effects on the solution. The boundaries for the inlet and outlet of the domain were chosen to be of a Dirichlet type with values given by the 1-D jump condition, while the boundaries bounding the y-direction were chosen as symmetry conditions. This allows us to use a computational domain that is half a cell's wavelength in the domain. Throughout the computational domain, a minimum refinement of 2 numerical cells per flame length is used with 4 levels of refinement available to the solver. A mesh level comparison is done at every time step to resolve the section of the mesh that requires more cells. Finally, to ensure that the reaction was resolved at all times, the maximum resolution of 32 grid points per unit length is used in the region where the progress variable Y is between 0.01 and 0.99.

It is interesting to define the Zel'dovich number, β as

$$\beta = \frac{QE_a}{(1+Q)^2}. \tag{6}$$

Four sets of parameters have been chosen for this study. The Zel'dovich number and heat release are both changed independently while $\gamma = 1.4$, $Le = 1$, $Pr = 0.75$ are kept constant.

Table 1: Important parameters for problems of interest.

Name	γ	Pr	Le	Q	β
Problem 1	1.4	0.75	1	6	5
Problem 2	1.4	0.75	1	6	10
Problem 3	1.4	0.75	1	9	5
Problem 4	1.4	0.75	1	9	10

Each of these parameters is studied for Mach numbers ranging from their quasi-isobaric flame velocities ($M_f = 0.005$) to their compressible Chapman-Jouguet (CJ) deflagration velocity (Case 1 & 2: $M_f = 0.18028$) and (Case 3 & 4: $M_f = 0.148777$).

The initial condition is set as an protrusion of the 1-D solution across the y-domain. In order to excite any instability, an initial perturbation of the x-direction of the 1-D flame profile of the form $A_0 \cos(2\pi y/\lambda)$ where $A_0 = 0.01$ is used.

For a given set of parameters and flame Mach numbers, the value of Λ is still unknown and has to be found iteratively. To do this, the solution of the 1-D problem is found using an implicit numerical solver. Only

once the correct value of Λ is found, a steady state solution for the given Mach number of the flame can be found. Figure 1 shows a comparison of the results of Case 1 re-dimentionalized using $\hat{p} = \frac{p}{\gamma M_1^2}$ and $\hat{T} = \frac{T}{\gamma M_1^2 (Q+1)}$. We notice that, while the quasi-isobaric and CJ deflagration flame profiles are similar, there are two significant differences. The first and most obvious is the pressure drop after the reaction zone in the CJ deflagration is more than half of the unburned pressure while in the quasi-isobaric case the drop in pressure is less than 1/10th of one percent. The second is that the increase in temperature is more significant in the quasi-isobaric profile due to the smaller pressure drop. There is also a peak in the temperature profile that appears for the higher-speed case.

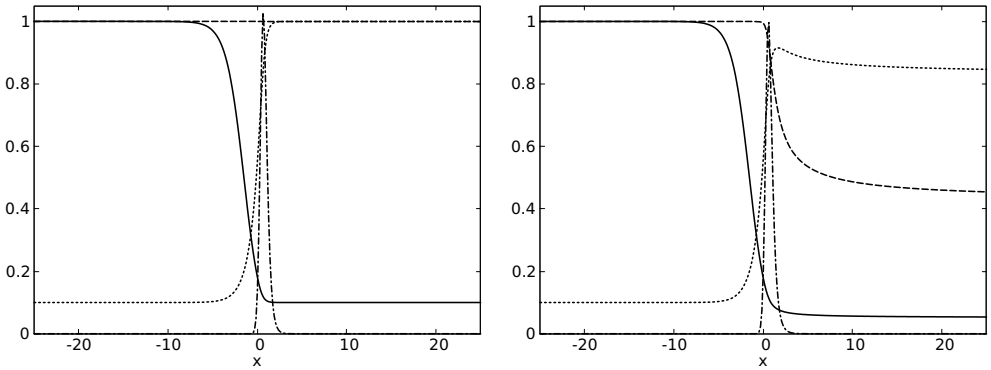

Figure 1: 1-D profile of Problem 3 for the quasi-isobaric case (left) and the fast flame (right): Density(——), Pressure(- - - -), Temperature(·····), Reaction Zone(– · – ·).

4 Numerical Results

This reaction model is not representative any specific real gas mixture due to its simplicity. These equations are, rather a tool to investigate the possible effects of instability in flames and the effects of changing macro-properties of reactions such as the energy of activation of a mixture and the heat release of reaction. Fast turbulent burning velocities are modelled using laminar profiles, with no turbulence. To achieve these fast flames, the velocity of the flame can be increased by increasing the pre-exponential factor of the Arrhenius reaction term. This increase in the rate constant of the reaction is intended to model an increased level of turbulence, and not a change in chemical kinetics. The reaction in the quasi-isobaric flames happens after the species diffusion zone is almost completed while, at the CJ deflagration speed, the reaction zone is at the front of the diffusion zone, this is correlated with a reaction zone that is affected by turbulence. A Lewis number of unity was also chosen to simulate a fast flame regime where propagation is strongly affected by turbulence, one can expect reduced significance of the effect of the thermodiffusive instability in such a situation.

Figure 2 depicts the flame speed in a frame of reference of the pre-shocked unbuned gas (V_{abs}). The flame speed calculated from the reaction rate ($V_r = \int W dx$) and the flame surface area (A_r). One can observe that the growth rate of the isobaric case is much slower than the fast flame. It is also notable that the increase in the reaction velocity in the fast flame is not proportional to the increase in the flame area, while in the quasi-isobaric case is similarly proportional. The increase in reaction rate of the flame with respect to the surface area of problem 3 is shown in Table 2 as well as the velocity of the flame in the pre-shocked unburned gas frame of reference.

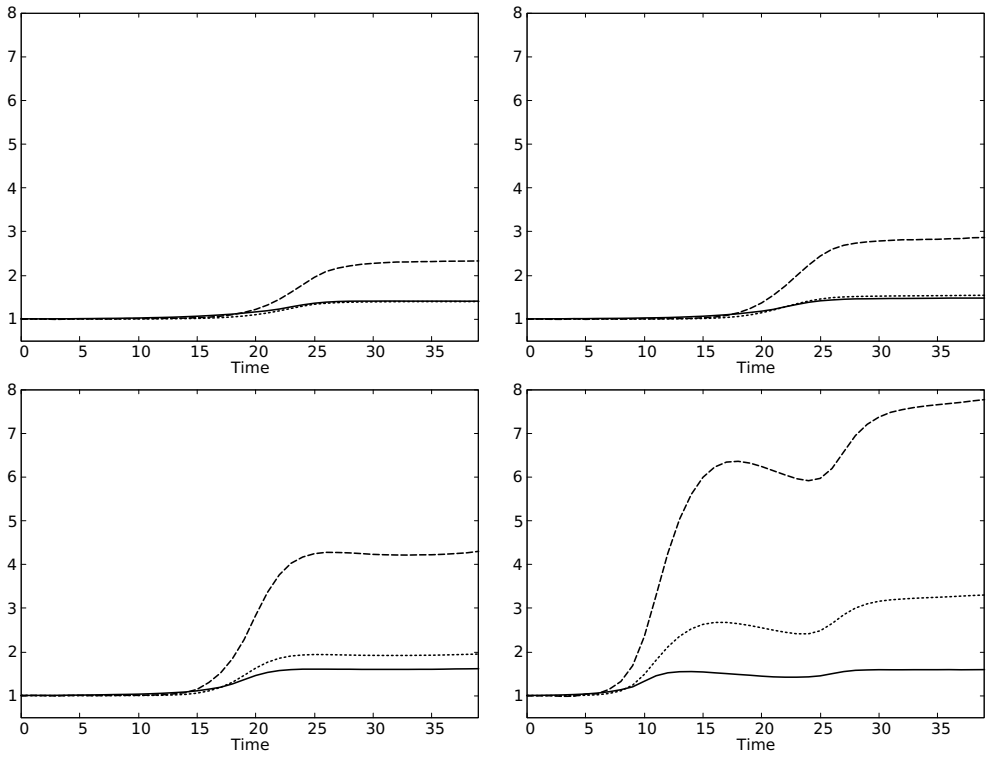

Figure 2: Reaction rates of Problem 3 for $M_f = 0.03$, $M_f = 0.07$, $M_f = 0.11$ and $M_f = 0.148777$: Flame surface area(——), Flame Velocity with respect to unperturbed unburned gas(- - - -), Turbulent burning velocity(·····).

Figure 3 shows the evolution of the density for Case 3 at a time of 0, 10, 20, 30 and 40. A significant compression zone appears in the unburned gas. This precompression of the gas could explain the increased reaction rates that we see in Figure 2 for the fast flame. We hypothesize that this precompression region has three significant effects on flame stability in the compressible regime. The first cause of instability is due to the pre-heated region caused by the pre-compressed gas in front of the flame. The simulation show that in early development of the cellular structure the compression is most notable in the convex section of the flame. This means that, due to the slight temperature rise, the precompression increases the flame velocity at the apex of the flame. This increases its growth rate until the precompression zone stabilizes through the domain at a later time. The precompression also has the effect of convecting the gas forward. In other words, the flame will then be convected forward by the increase of velocity in the pre-compressed region. This can explain the difference between the velocity of the flame in the stationary frame of reference and the velocity of the flame calculated by the reaction rate. Finally, we would expect that the flame would have more difficulty expanding in a denser region, so that the denser pre-compressed area would slow down the growth rate of the cells. The interaction between these three effects and the Darrieus-Landau instability is a very difficult problem to separate. Table 3 shows the percent increase in conserved properties in the precompression region denoted by the subscript ”s”, as expected the precompression region increases in strength as flames propagate faster.

Table 2: Flame velocity with respect to the reaction surface area.

M_f	V_r/A_r	V_{abs}/A_r
0.03	0.99	1.65
0.07	1.04	1.93
0.11	1.20	2.66
M_{CJ}	2.06	4.86

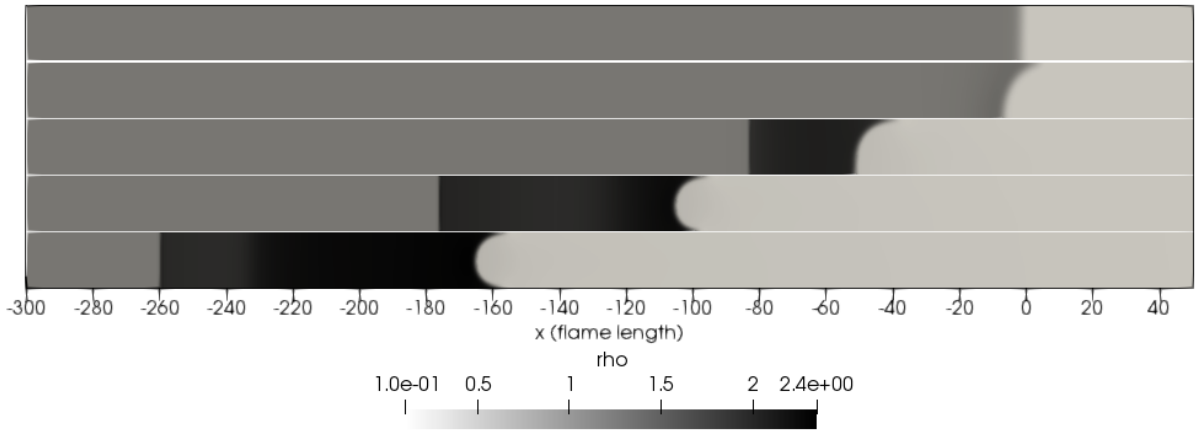

Figure 3: Density Evolution of Fast Flame for problem 3

4 Vorticity Evolution in Flames

Due to compressibility and density change, vorticity production is prominent in the flame structure of cellular deflagration. An analysis of the vorticity as well as the terms in the vorticity equation is done for all four problem stated.

Vorticity is an indication of the areas where turbulence is also expected to be prominent, it can also help isolate other important flow characteristics. Vorticity defines the local rotation of the fluid compared to the continuum and can be measured using

$$\omega_i = e_{ijk}\frac{\partial v_k}{\partial x_j}. \tag{7}$$

Since vorticity is a manifestation of angular momentum, we can analyze the evolution for vorticity by taking the curl of the momentum equation,

$$\frac{\partial \omega_i}{\partial t} = \underbrace{-v_j\frac{\partial \omega_i}{\partial x_j}}_{\text{Convection}} + \underbrace{\omega_j\frac{\partial v_i}{\partial x_j} - \omega_i\frac{\partial v_j}{\partial x_j}}_{\text{Deformation}} + \underbrace{e_{ijk}\frac{1}{\rho^2}\frac{\partial \rho}{\partial x_j}\frac{\partial p}{\partial x_k}}_{\text{Baroclinicity}} + \underbrace{e_{ijk}\frac{\partial}{\partial x_j}(\frac{1}{\rho}\frac{\partial \tau_{km}}{\partial x_m})}_{\text{Viscous}}. \tag{8}$$

There are four processes that can lead to a change in the local vorticity. The vorticity can be convected by the background flow velocity. Deformation can be important, however in a 2 dimensional flow the $\omega_j\frac{\partial v_i}{\partial x_j}$ is zero due to vorticity only existing in the z-direction. We can also get vorticity concentration or dilution due to flow accelerating or decelerating. The baroclinicity is a source of vorticity due to the misalignment of density and pressure gradients, we can imagine that this effect will be more prominent in the compressible

Table 3: precompression jump in primitive variables.

M_f	ρ_s/ρ_1	T_s/T_1	p_s/p	u_s
0.03	1.03	1.00	1.00	0.01
0.07	1.11	1.04	1.15	-0.47
0.11	1.35	1.13	1.53	-1.86
V_{CJ}	2.31	1.44	3.30	-5.33

regime than the incompressible regime. We can also have vorticity production due to the viscous stresses, these effects are normally strongest in the boundary layers or shear layers.

Figure 4 shows the evolution of vorticity of Problem 3 at the same times as defined for Figures 3. The vorticity in these plots are concentrated on the cusps of the cellular profile, while the convex section of the flame does not have significant vorticity.

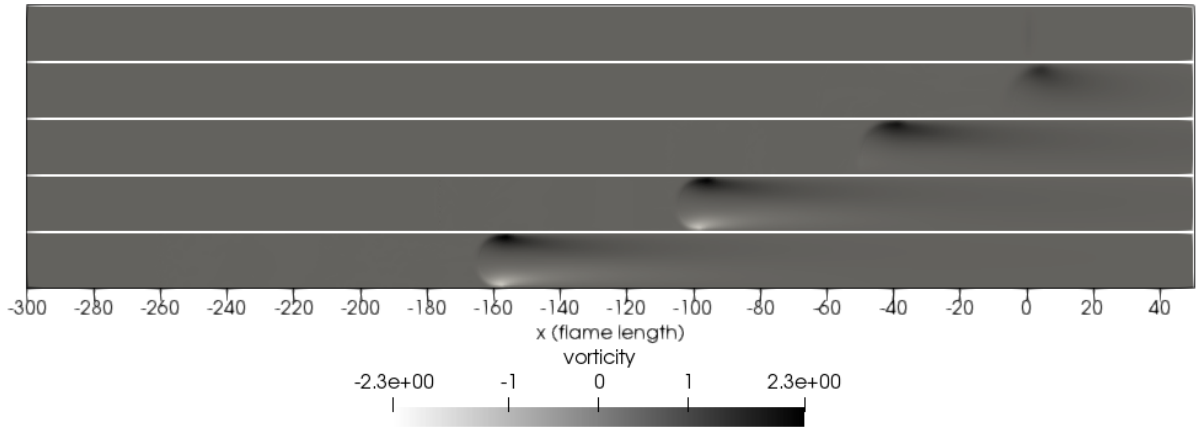

Figure 4: Vorticity Evolution of fast flame for Problem 3

Matalon [16] showed that the DL instability also predicted that the vorticity in perturbed flames would increase the instability. Figure 4 depicts visually this effect, where, on the left the positive rotation of vorticity in this section of the flame would have a stabilizing effect, while a negative rotation shown on the right would have a destabilizing effect. The solution to the chosen model shows that the vorticity rotation that has been produced once the flame thickness is taken into consideration is expected to have a stabilizing effect.

It is also interesting to see the effects of each individual term in the evolution equation for the vorticity for the different flame velocities. Figure 6 shows the summation of each term in the vorticity equation in a moving frame of reference with the flame in a domain of ± 10. We can see the general effect of increasing the Mach number of the flame is an increase in vorticity production, we also notice that the convection and the viscous term in the equation are non-zero but have minimal effect on the vorticity when compared to the baroclinic source and the deformation sink.

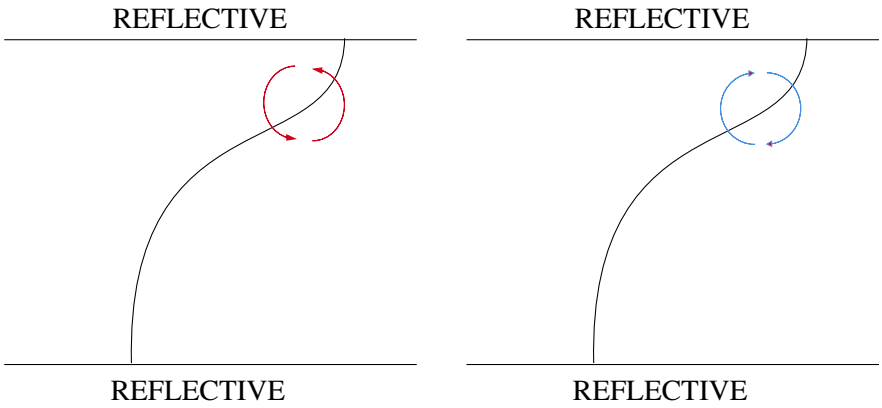

Figure 5: Vorticity rotation effects on the flame.

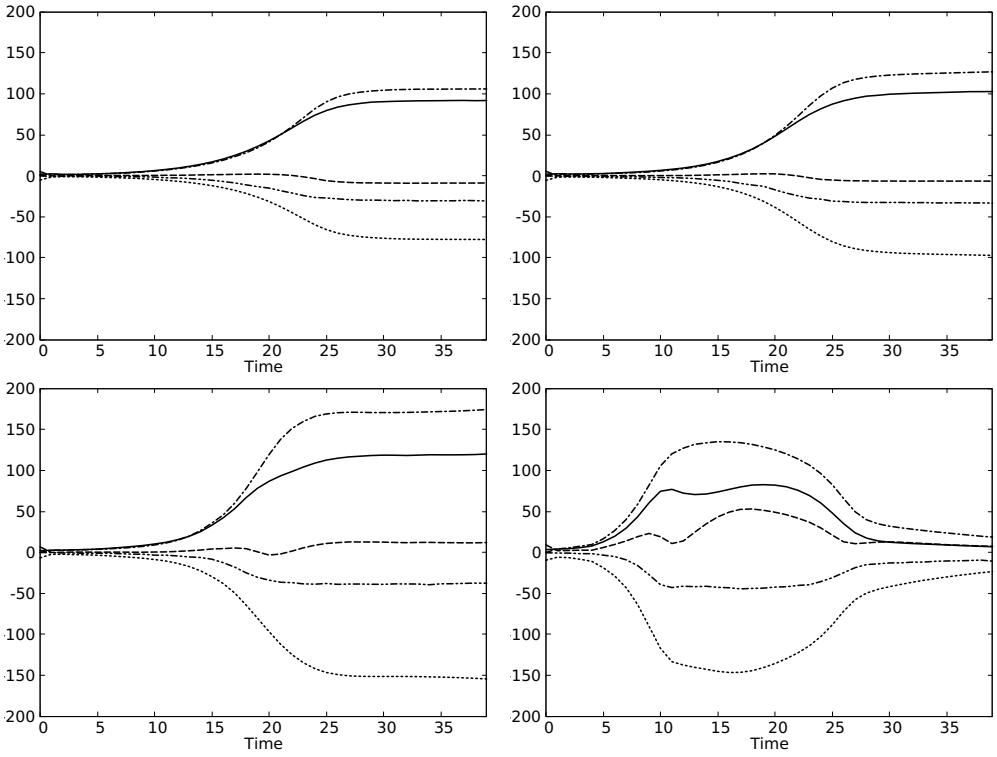

Figure 6: Vorticity equation terms evolution in time for Problem 3 with flame Mach number 0.03, 0.07, 0.11 and M_{CJ}: Total Vorticity(——), Convection(- - - -), Baroclinic(— · — ·), Deformation(·····), Viscous(— — —).

5 Conclusion

The two-dimensional evolution of fast flames using the Navier-Stokes equations with a one-step chemistry model was evaluated. It was found that, compared with the quasi-isobaric flames, fast flames produce a significant precompression region affecting the growth rate of the flames. The reaction velocities in flames compared to the flame area are found to be 0.99, 1.04, 1.20 and 2.06 for flame Mach numbers of 0.03,

0.07, 0.11 and 0.14877. An increase of 1.65, 1.93, 2.66 and 4.86 was also found when considering the flame velocity in the frame of reference of the unburned gas. The results also show that CJ flames do not stabilize as predicted by Bychkov [14] and He [13]. Three possible cause of the increase of instability due to compressibility are proposed. The first is the increase of reaction rate in the convex section of the flame due to the pre-heating, the second is the convection of the convex section of the flame due to the unburned gas velocity and finally the increase density as a stabilizing effect is proposed. Further analysis of the vorticity showed that the baroclinic source term is the prominent source of vorticity production in flames and that there is an increase of vorticity in faster flames.

References

[1] G. Darrieus, "Propagation d'un front de flamme," 1938. La Technique Modèrne (Paris) and in 1945 at Congres de Mécanique Appliquée.

[2] L. Landau, "The Darrieus-Landau instability in fast deflagration and laser ablation," *Acta Physicochim*, vol. 19, no. 77, 1944.

[3] P. Clavin and F. A. Williams, "Effects of molecular diffusion and of thermal expansion on the structure and dynamics of premixed flames in turbulent flows of large scale and low intensity," *Journal of Fluid Mechanics*, vol. 116, no. -1, pp. 251–282, 1982.

[4] P. Pelce and P. Clavin, "Influence of hydrodynamics and diffusion upon the stability limits of laminar premixed flames," *Journal of Fluid Mechanics*, vol. 124, no. -1, pp. 219–237, 1982.

[5] Liberman, Bychkov, Golberg, and Book, "Stability of a planar flame front in the slow-combustion regime," *Physical review. E, Statistical physics, plasmas, fluids, and related interdisciplinary topics*, vol. 49, no. 1, 1994.

[6] O. Y. Travnikov, M. A. Liberman, and V. V. Bychkov, "Stability of a planar flame front in a compressible flow," *Physics of Fluids*, vol. 9, no. 12, pp. 3935–3937, 1997.

[7] G. Sharpe, "Linear stability of planar premixed flames: reactive Navier-Stokes equations with finite activation energy and arbitrary lewis number," *Combustion Theory And Modelling*, vol. 7, pp. 45–65, March 2003.

[8] G. J. Sharpe and S. A. E. G. Falle, "Nonlinear cellular instabilities of planar premixed flames: numerical simulations of the reactive Navier-Stokes equations," *Combustion Theory and Modelling*, vol. 10, pp. 483–514, June 2006.

[9] O. Y. Travnikov, V. V. Bychkov, and M. A. Liberman, "Influence of compressibility on propagation of curved flames," *Physics of Fluids*, vol. 11, no. 9, pp. 2657–2666, 1999.

[10] S. Kadowaki, "Numerical study on lateral movements of cellular flames," *Physical Review E - Statistical Physics, Plasmas, Fluids, and Related Interdisciplinary Topics*, vol. 56, no. 3, pp. 2966–2971, 1997.

[11] S. Kadowaki, "The lateral movement of the three-dimensional cellular flame at low lewis numbers," *International Journal of Heat and Fluid Flow*, vol. 20, no. 6, pp. 649–656, 1999.

[12] S. Kadowaki, "Numerical study on the formation of cellular premixed flames at high lewis numbers," *Physics of Fluids*, vol. 12, no. 9, pp. 2352–2359, 2000.

[13] L. He, "Analysis of compressibility effects on Darrieus-Landau instability of deflagration wave," *EPL (Europhysics Letters)*, vol. 49, no. 5, pp. 576–582, 2000.

[14] V. Bychkov, M. Modestov, and M. Marklund, "The Darrieus-Landau instability in fast deflagration and laser ablation," *Physics of Plasmas*, vol. 15, no. 3, 2008.

[15] S. A. E. G. Falle and J. R. Giddings, "Body capturing using adaptive cartesian grids, in numerical methods for fluid dynamics iv," pp. 337–343, 1993.

[16] M. Matalon, "The Darrieus-Landau instability of premixed flames," *Fluid Dynamics Research*, vol. 50, no. 5, 2018.